Coherent Ultra Dense WDM Technology for Next Generation Optical Metro and Access Networks

Harald Rohde, *Senior Member, IEEE*, Erich Gottwald, Antonio Teixeira, Jacklyn Dias Reis, Ali Shahpari, Klaus Pulverer, and Jun Shan Wey, *Senior Member, IEEE*

***Abstract*—Coherent optical communication has been well established as the technology of choice for long haul and high bit rate communication systems since a decade ago. Recent technology advances and ongoing price erosion further open the window of opportunity for the application of coherent optical transmission technology in other domains. This paper describes in detail the capabilities, design and implementation of a coherent ultra dense WDM technology for optical metro and access networks. Its capabilities enable a number of attractive options, such as variable downstream bit rates from 150 Mbit/s up to 10 Gbit/s per user, embedded OTDR and the coexistence with legacy systems such as GPON, EPON, XGPON or RF-Video in optical distribution networks. Due to its flexibility and capacity, it is also suitable for deployments in metropolitan networks, as well as for mobile front-haul and back-haul applications.**

***Index Terms*—Communication systems, optical fiber communication, optical modulation.**

I. Introduction

THE basic ideas of coherent reception in the form of heterodyne radio receivers date back almost 100 years when the first technical realizations were implemented around 1918. Heterodyne radios are superior to direct detection radios in terms of sensitivity and frequency selectivity. Because of this reason, optical heterodyne reception (synonym of "coherent reception") was a hot topic [1] in the early development phase of optical communication systems until the advent of EDFA rendered coherent transmission obsolete in late 1980 [2]. Requirements such as high spectral efficiency at high data rates and electronic dispersion equalization brought optical coherent transmission back. Nowadays, coherent transmission is used in numerous single wavelength 40 Gbit/s deployments and in all single wavelength 100 Gbit/s installations. A good introduction to the general coherent reception concept is given in [3].

It is envisioned that coherent optical transmission follows the trend migrating from the high margin, low volume long haul market into the low margin, high volume metro and access arena. It is expected to first reach the metro network market with main applications in access backhaul, mobile backhaul, and connectivity for small and medium enterprises, followed by penetrating into the Fiber to the Home/Curb/Building/Cabinet market. In the ideal case, each connected user is assigned a unique wavelength, so the number of wavelengths has to be high in order to connect a suitable user base per feeder fiber. This leads to the development of Ultra Dense WDM (UDWDM) systems with wavelength spacings as low as 2–3 GHz [4]. The high wavelength selectivity of a coherent receiver enables the use of such a dense spacing without highly elaborated wavelength filters.

Early experiments of ultra dense coherent optical metro and access systems described the generation and detection of an ultra dense wavelength grid with conventional laser arrays, wavelength combiners and cascaded wavelength filters [5]. Initial ideas about coherent access have been around since 80's [6]–[9], industry picked it up in recent years [4], [10].

Standardization is an important aspect for new technology introduction into the market and support of a healthy ecosystem. Standardization of a pure WDM access networks was first discussed in the early 2000. However, it was not until 2010, when the pre-standardization work on NG-PON2 began in the Full Service Access Network forum, that a pure WDM access system was taken seriously. For access networks, a tunable point-to-point WDM solution is included as an option in the ITU-T G.989 series Recommendation. Two ODN topologies, legacy power-splitter-based and AWG-based in green field, are supported. UDWDM as proposed in this paper supports both topologies [11]. For metro applications, discussion for a low-cost WDM metro system has also started in ITU-T Question 6/Study Group 15.

This paper describes the design, basic working principle, and detail implementations of the real-time optical line terminal (OLT) and optical network unit (ONU) of an UDWDM system. The techniques to achieve flexible bit rates from 150 Mbit/s to 10 Gbit/s and to implement an embedded OTDR are discussed. Numeric simulations of system limitation caused by fiber nonlinearities, as well as experimental results of transmission of UDWDM in the presence of legacy systems are presented. Note that although for simplicity terminologies specific to access networks are used throughout this paper, the

Manuscript received August 20, 2013; revised February 5, 2014 and March 20, 2014; accepted April 2, 2014. Date of publication April 9, 2014; date of current version May 12, 2014.

H. Rohde, E. Gottwald, and K. Pulverer are with the Coriant GmbH, 80240 Munich, Germany (e-mail: Harald.Rohde@coriant.com; erich.gottwald@coriant.com; klaus.pulverer@coriant.com).

A. Teixeira and A. Shahpari are with the Instituto de Telecomunicações, Universidade de Aveiro, 3810-193 Aveiro, Portugal (e-mail: teixeira@ua.pt; Ali@ua.pt).

J. D. Reis is with CPqD, Campinas-SP 13086-902, Brazil (e-mail: jacklyn@cpqd.com.br).

J. S. Wey is with the Coriant Americas, Redmond, WA 98052 USA (e-mail: shan.wey@nsn.com).

Color versions of one or more of the figures in this paper are available online at http://ieeexplore.ieee.org.

Digital Object Identifier 10.1109/JLT.2014.2316369

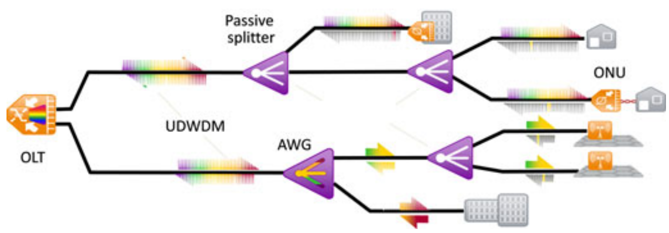

Fig. 1. Basic system design.

same concept and implementationx apply directly for metro networks.

II. System Design and Capabilities

An example of a basic coherent UDWDM network design is given in Fig. 1. An OLT generates multiple wavelengths in an ultra-dense wavelength grid. The specific wavelength spacing, typically at about 3 GHz, will be explained in Section III. All wavelengths are transmitted on the same standard single mode fiber (SSMF). The light on that fiber is then distributed equally to all branches of the PON tree if there are only wavelength agnostic passive splitters in the distribution network (ODN) as shown in the upper path of Fig. 1. It is also possible to use wavelength filters, such as arrayed waveguide gratings (AWGs), in the distribution node in order to select specific wavelength bands (see Fig. 1, lower path). The optical insertion loss of AWGs is lower than that of passive splitters for split factors higher than 8, thus longer reach distance can be realized when using AWGs in the ODN. Potential privacy issues are better addressed with the use of AWGs because of the assignment of specific wavelength bands to different users.

Depending on the ODN configuration, each user receives all wavelengths or a subset thereof. Each ONU is fully tunable in the C-band and detects only the intended wavelength by means of coherent reception. Each wavelength carries 1 Gbit/s payload. Data rate per user can be selected between 150 Mbit/s and 10 Gbit/s based on the technique described in Section IX. Privacy is ensured by encryption at the data layer. The high sensitivity of coherent reception allows for an optical loss budget of 43 dB which can be traded arbitrarily between reach and split. Depending on the ODN configuration, this power budget allows the connection of up to 1000 users with a reach of up to 100 km.

The number of parallel users is limited by the total optical power launched into the fiber, as explained in Section VII. Up to 240 wavelengths with -2 dBm/wavelength can be transmitted without violating eye safety regulation; for larger numbers, an automatic laser shutdown circuit is required or lower power per wavelength can be launched. In this work, the experimental operation of 960 wavelengths is shown, and in [12] 1008 wavelengths were propagated through a similar ODN. Due to the low per wavelength launched power, the effect of non-linear interactions such as Raman is limited (e.g. with 960 wavelengths at -2 dBm and 20 km the maximum power variation among wavelengths, due to static Raman, is 5 dB, and 0.6 dB for -10 dBm per wavelength) and should be subject to further studies. Nonlinear effects related to other UDWDM wavelengths are discussed in Section X, and impairments of external (coexisting) systems in Section XI.

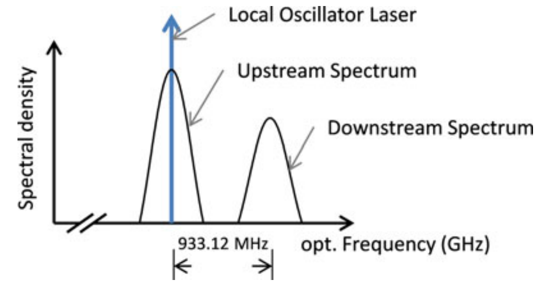

Fig. 2. Spectral position of the downstream and the upstream wavelength in the ONU.

III. Basic Working Principle: Paired Channel Technology

In a straightforward implementation, the ultra-dense wavelength spacing requires the use of highly precise and stable external wavelength lockers in the ONU, which cannot be implemented cost effectively. An innovative implementation called "Paired Channel Technology" (PCT) is introduced as a practical and economical way to generate very closely spaced wavelengths without using wavelength lockers. The key idea of the PCT is to lock the upstream wavelength to the received downstream wavelength of which the relative spectral position is shown in Fig. 2. The detection and locking of the downstream wavelength relies on coherent reception by use of a tunable local oscillator (LO) laser in the ONU. Part of the LO laser light is modulated and used as the upstream signal. Note that a system which uses exactly the same wavelength for upstream and downstream in a single fiber configuration would be very sensitive to back reflections from the ODN. To minimize the effect of back reflections, the upstream wavelength is detuned from the downstream wavelength by $+933.12$ MHz for payload up to 1 Gbit/s. The reason for the frequency choices in this section is explained in detail in Section IV.

Note that throughout the paper the terms "frequency" and "wavelength" are used interchangeably for the convenience of description.

On the OLT side, it would be highly impractical and expensive to use 1000 lasers which are all locked to the respective, ultra fine grid. Therefore, the practical solution is to generate multiple wavelengths out of a single laser source that also serves as a LO for the coherent reception of the corresponding upstream wavelengths. Such a unit, generating and receiving 10 wavelengths, is called Optical Transceiver Group (OTG) and further explained in Section V. Fig. 3(a) shows the spectral position of the downstream wavelengths of an OTG, the corresponding upstream wavelengths, and the respective back reflections. The frequency is scaled in units of $\Delta = 933.12$ MHz. The two downstream wavelengths with the smallest frequency deviation from the originating carriers have a spectral distance from the carrier of $2\Delta = 1866.24$ MHz (resulting in a total distance of 4Δ) while all other wavelengths have a spectral distance of $3\Delta = 2799.36$ MHz.

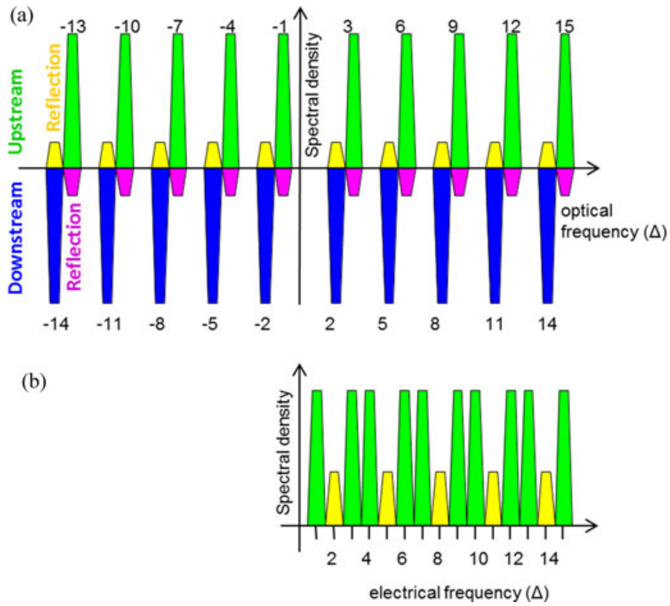

Fig. 3. (a) Wavelength scheme of one Optical Transceiver Group, Transmit direction. (b) Electrical spectrum at the OLT receiver. All frequencies are denoted as multiples of $\Delta f = 933.12$ MHz.

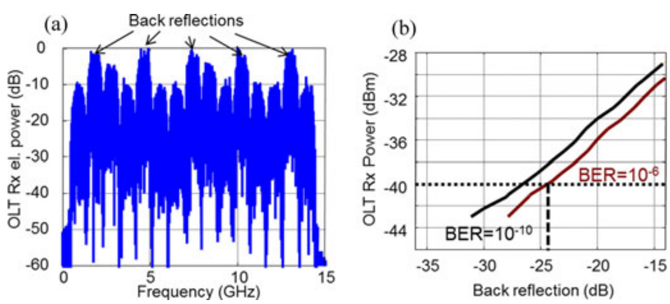

Fig. 4. (a) Simulated OLT Rx electrical spectrum, (b) Simulated BER versus back reflection level.

Fig. 3(a) illustrates the wavelength scheme generated by one OTG. The blue downstream spectrum is symmetric with respect to the central LO frequency and causes back reflections indicated by the yellow bars. The green upstream spectrum is chosen so that these back reflections can be filtered efficiently in the electrical domain. At the OLT, the upstream wavelengths are superimposed with the LO laser and detected by a balanced pair of photodiodes. This effectively "folds over" the spectrum as illustrated in Fig. 3(b). The yellow garbage bands containing back reflections from the left and right sides of the downstream spectrum coincide, so that only 1/3 of the electrical spectrum needs to be filtered.

Fig. 4(a) shows as an example the simulated electrical spectrum at the input of the OLT receiver as outlined in the wavelength scheme in Fig. 3(b). In this specific case with signal levels close to receiver sensitivity, the back reflections have higher amplitude than the payload signal, but due to the pulse shaping (see Section V) and the resulting spectral separation, relatively high back reflection levels can be tolerated.

Fig. 4(b) shows the dependence of the optical input powers at OLT Rx for given BERs versus back reflection. It can be seen that for a BER of 10^{-6} and an OLT Rx input power of -40 dBm, about -24 dB of back reflection can be tolerated. The back reflections stem from Rayleigh back scattering, back reflections at connectors and other optical components. A full noise chain, including laser linewidth of the transmitter and receiver, laser relative intensity noise, shot noise, electrical noise and optical amplifier noise has been included in the calculation. A detailed analysis of back reflections can be found in [13].

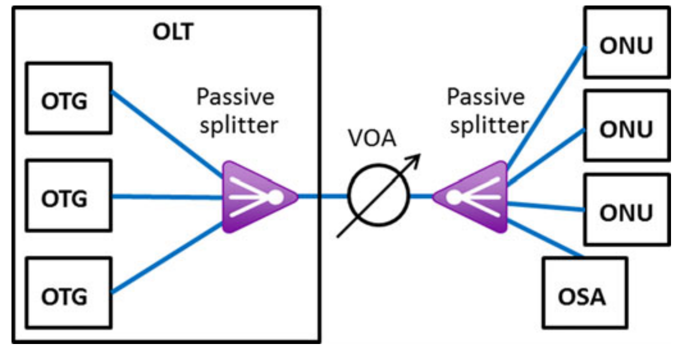

Fig. 5. Experimental setup.

The viability of PCT is demonstrated with the prototype setup shown in Fig. 5. The OLT consists of three OTGs each generating 10 wavelengths, which are combined with a passive splitter. To simulate variable reach, measurements are performed using a variable attenuator. This is validated by transmitting the signals over 40 km of standard single mode fibre and observing no difference in the behavior between using fibre and the equivalent attenuator value. Behind the downstream splitter stage, three independent ONUs can tune freely across the available spectrum and lock on to an assigned downstream signal. The results described in this paper were taken with an OSA located in parallel to the ONUs.

IV. Clocks, Frequencies and Frequency Relations

The frequencies in the system are selected to make data processing as efficient as possible. To this end, all clocks and frequencies in the system, including the wavelength spacing, are integer multiples of a base frequency. This base frequency is chosen to be STM 1 at 155.52 MHz.

The data rate of 1244.16 MHz is 8 times the base frequency (i.e. STM 8). As DQPSK with two bits per symbol is used as modulation format, the symbol rate is 622.08 MHz. The base unit for the wavelength spacing is six times the STM 1 rate, i.e., 933.12 MHz. Such a frequency slot can host a 622.08 Mbaud signal with a square root raised cosine pulse shaping (roll off = 0.5) and leave some room for laser drifts (see Sections V and VI)

In the OLT transmit direction, the high speed digital to analog converters run at 57.71968 GSamples/s which equals 384 times the STM 1 frequency or 64 times the wavelength spacing Δf.

The ONU receiver analog-to-digital (ADC) converters sample at 3.73248 GSamples/s which equal 24 times the STM-1 rate. As heterodyne reception with an intermediate frequency of 933.12 MHz is used (see Sections V and VI), the ADC sampling

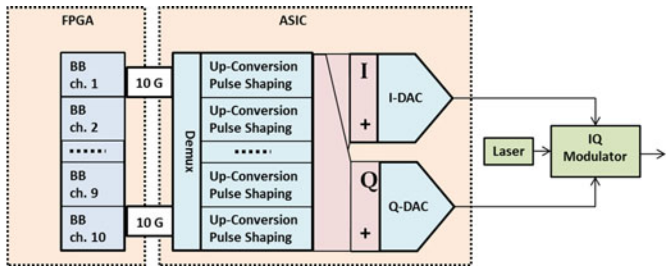

Fig. 6. OLT transmit path block diagram.

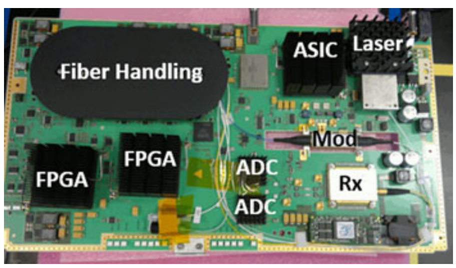

Fig. 7. OLT prototype board.

rate equals four times the intermediate frequency. This enables efficient digital down-conversion algorithms, as discussed in Section VI.

V. Real Time OLT

The block diagram of the transmit path of one OTG of a real time UDWDM OLT is shown in Fig. 6. In this implementation, one single laser is needed to generate 10 wavelengths.

The prototype board is shown in Fig. 7. An FPGA performs the baseband processing to generate 1.24416 Gbit/s data streams out of a 1 Gbit/s Ethernet signal for each of the 10 wavelengths. The FPGA also performs framing, forward error correction (FEC) encoding, and functions such as differential encoding and scrambling of the bit streams. The resulting 10 bit streams, each at 1.24416 Gbit/s, are then transferred into an ASIC, which consists of 10 parallel up-conversion, pulse shaping blocks, and a pair of digital-to-analog converters (DACs). The up-converters transfer baseband data onto high frequency, DQPSK modulated carriers. The carrier frequencies are integer multiples of the base frequency unit of 933.12 MHz. The carrier frequencies are $\{-14, -11, -8, -5, -2, 2, 5, 8, 11, 14\}*933.12$ MHz.

In the ASIC, the high frequency carriers are represented as 8-bit data streams for both the In-Phase ("I") and the Quadrature ("Q") components. In order to have a clear separation of the wavelengths, a square root raised cosine pulse shaping filter (roll-off factor = 0.5) is applied. On the receive side, the same filter is applied so that the resulting function corresponds to a raised cosine filter. The I and Q components of all high frequency carriers are then added and converted into electrical currents by two high speed DACs at a sampling rate of 59.72 GSamples/s ($=64 \times 933.12$ MHz).

The two output currents from the high speed DACs are then amplified and used to drive an IQ-modulator which modulates the light from a narrow linewidth laser. The laser linewidth is less

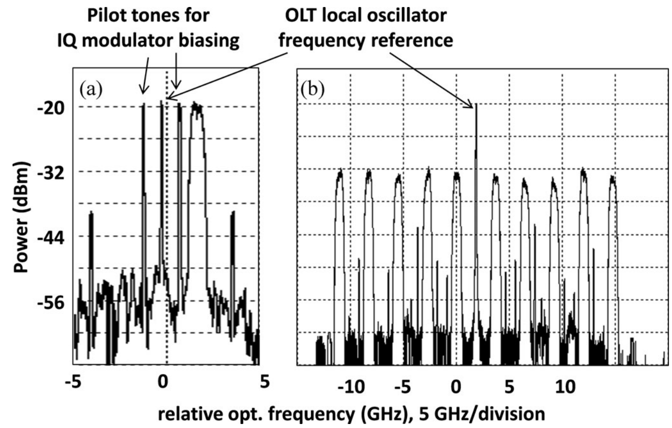

Fig. 8. Experimental output spectra of the OLT transmit block. (a) One active wavelength, (b) 10 active wavelengths.

than 100 kHz throughout the whole C band tuning range. The IQ modulator is operated such that it generates single sideband signals. Each of the 10 electrical channels generates its own single sideband signal so that each resulting wavelength is individually modulated with a pulse shaped 622 Mbaud DQPSK signal. Fig. 8 depicts the generated spectra at the output of the OLT transmitter, measured using a high resolution optical spectrum analyzer with a resolution of 20 MHz. The amplitude of each wavelength is pre-emphasized to compensate for the frequency dependence of the RF driving path from the ASIC to the modulator.

In order to demonstrate and verify the single sideband operation, only one carrier is active in Fig. 8(a). It can be seen that the sidebands are suppressed by about 30 dB. The residual carrier is visible as well as two pilot tones at ± 933.12 MHz which serve for the adjustment of the right biasing of the IQ modulator. In Fig. 8(b), all 10 wavelengths were activated while the pilot tones were switched off. The narrow, small spectral lines close to the payload wavelengths are caused by residual clock spurs of the DAC. They carry negligible energy and do not cause a negative effect on the system performance.

Practical implementations of coherent receivers have been described extensively [14], [15] and will not be repeated here. On the receive side of the OLT, a polymer wideband polarization diverse coherent receiver is used. The same laser which generates the 10 downstream wavelengths is used as a LO for the reception of the 10 upstream wavelengths. For the upstream, a pair of 60 GSamples/s ADCs is intended to digitize the signals. The data streams are then filtered and down-converted in parallel by a weighted overlay and add structure [16], [17] and received by a bank of 10 parallel 1.24416 Gbit/s DQPSK decoders, un-framers and FEC units.

The FEC units are implemented and have been used for data transmission such as HD-Video or LTE backhauling, however, for all BER measurements throughout this paper FEC has been deactivated. A G.709 standard (RS 255,239) FEC has been implemented. The payload data is 1G Ethernet which is mapped into an OTU 0 frame structure.

As at this time the 60 GSamples/s ADC is still under development, an intermediate OLT receiver digital signal processor

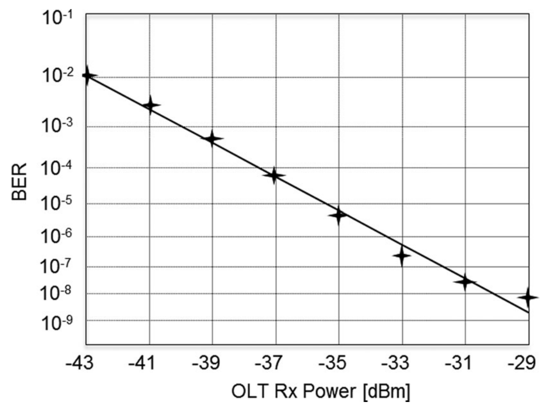

Fig. 9. Bit Error Rate curve for the OLT.

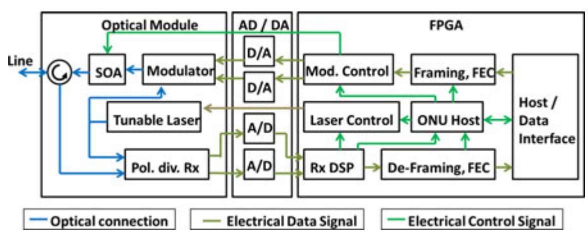

Fig. 10. Block diagram of the ONU.

(DSP) unit has been implemented using wideband optics capable of receiving all 10 upstream wavelengths. However, this intermediate DSP unit only consists of one pair of 4 GSamples/s ADCs and thus is only able to receive one upstream wavelength. Nevertheless, on the DSP side the full algorithms for the 10 wavelength reception have been implemented. The resulting bit error curve is shown in Fig. 9. The OLT receiver module sensitivity without optical pre-amplification for this setup is about -40 dBm for a bit error rate (BER) of 10^{-3}. This relatively low sensitivity is due to the low responsivity of the experimental polymer optical receiver which has about 10 dB of excess insertion loss compared to the commercially available InP based receivers. Without this excess loss, an OLT receiver sensitivity of about -50 dBm is expected from theoretical calculations and might be verified when such a receiver is available in the author's lab.

VI. Real Time ONU

The ONU consists of an integrated optical module, a FPGA, and a set of ADC/DAC as interfaces between the optical module and the FPGA. As shown in Fig. 10, the optical module [18] consists of a tunable laser, a polarization diversity receiver, an IQ modulator, and a variable optical attenuator (VOA) as upstream transmit power control. The tunable laser covers the full C band with a linewidth of <500 kHz over the full band. This leads to a phase error in the differential decoding of less than 3° for the used symbol rate of 622 Mbaud. Due to the differential decoding and a high speed phase tracking section in the DSP, low frequency phase noise components do not influence the BER. The polarization diversity receiver is configured as a heterodyne receiver with a heterodyne frequency of about 1 GHz and is equipped with low noise, linear transimpedance amplifiers. The IQ modulator performs the DQPSK modulation. An SOA serves as a VOA as well as a transmit power booster in order to either switch off the upstream light when the ONU is scanning or to set the right level of upstream transmission mode.

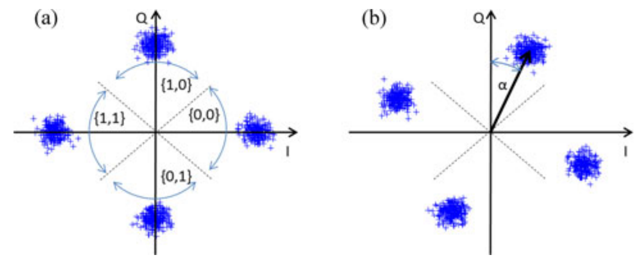

Fig. 11. Differential angle constellation used for tunable laser control: (a) Tunable laser perfectly tuned, (b) Tunable laser detuned by $\sim$40 MHz.

The output signals from the polarization diversity receiver are amplified and digitized by a pair of 3.8 GSamples/s, 8 bit ADCs and then fed into the FPGA receiver DSP, where clock recovery, polarization combination, compensation of fast laser phase fluctuations, and recovery of the differential phase angles of the transmitted signal are performed. According to the corresponding differential phase angle, bit pairs are generated and combined to a continuous bit stream. In the De-Framing block, a 'frame hunter' scans the received bit stream until a 'frame start' pattern is detected and then determines the correct byte alignment. The subsequent blocks perform de-scrambling and FEC decoding, and delivers the data stream to the data interface.

For the upstream path, the data is framed, scrambled and FEC-, and differentially encoded. A Modulation Control unit translates the stream of bit pairs (for the DQPSK modulation) into 14-bit values for the dual 2.4 GSamples/s, 14-bit transmit DACs which then drive the upstream IQ modulator.

An important task of a coherent optical receiver is the control of the LO laser, which must be in a relatively fixed spectral position with regard to the downstream light. The LO can be tightly locked to the optical phase of the downstream laser using optical phase-lock loop (OPLL) techniques. However, OPLLs, which require fast detection of the laser phase deviations and quick feedback to the LO, are rather expensive and complicated to implement [19]. Another technique is to tune the LO close enough to the downstream wavelength (or with a certain offset in the case of heterodyne reception) and then use DSP algorithms to detect and compensate for the fast laser phase fluctuations. In this case, the LO is only loosely locked to the downstream wavelength, which eases the requirements, thus the complexity and cost, for the LO tuning feedback loop. The ONU described in this paper uses the latter, i.e. the DSP tuning technique. The DSP algorithms are capable to compensate for LO offset frequencies of about ± 80 MHz. Part of this tolerance is based on the threshold settings of the angle detectors. Additionally a phase compensator is implemented which rotates the detected phases by multiplying the detected complex signal by $e^{-i\alpha}$, α being the phase due to the laser offset, as explained below.

Fig. 11(a) shows the detected differential angles when the LO and the downstream signal are perfectly tuned to the target

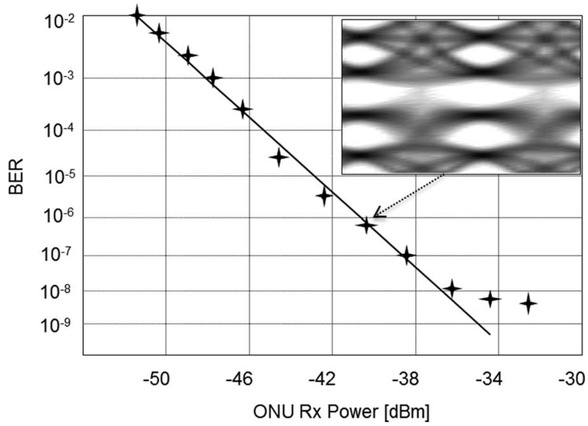

Fig. 12. Bit error curve for the ONU; Inset: Eye diagram at ONU.

difference frequency of 933.12 MHz. The angles have a certain distribution due to noise but can be all clearly assigned to bit pattern bins. Differential angles between -45° and 45° corresponds to a $\{0,0\}$ bit pair, between 45° and 135° correspond to $\{1,0\}$, and so on. If the LO laser is detuned, the optical relative phase between two symbols does not change by multiples of 90°, but is off-set by an angle α due to the additional rotation of the phase during the symbol time, as shown in Fig. 11(b). The frequency offset Δf is proportional to the symbol frequency times the offset angle in radian. For the example shown here, Δf = 622 MHz $\times$ $\alpha/2\pi$. The DSP calculates the average α angle and re-tunes the tunable laser if the resulting frequency offset exceeds 10 MHz. With this method, locking of the tunable laser to the downstream wavelength has been achieved for many hours.

Initial locking is achieved by a rough scan of the tunable laser over the wavelength band where downstream signals can be expected. When the tunable laser is within a few 100 MHz to a downstream wavelength, the amplitude at the output of the coherent detector would increase. When the amplitude crosses a certain threshold, the ONU starts a fine scan and steps the tunable laser in intervals of $\sim$10 MHz. The decoder stages of the DSP are active and deliver a received bitstream. If the frequency of the tunable laser is outside the allowed detuning range of $\sim\pm$80 MHz, the bitstream delivered by the DSP decoder contains just random data. After each tuning step, a "frame hunter" block tries to match the bitstream with the standard frame delimiter pattern "0xF6F6F6282828" defined in ITU-T G.709. If this pattern is found, the tunable laser is within the DSP processing range and fine tuning is applied.

The BER curve can be seen in Fig. 12. A sensitivity of about -48 dBm for a BER of 10^{-3} was measured. An optical power budget of 46 dB is achieved considering a per wavelength launch power of -2 dBm. Fig. 12, inset, shows a typical 4 level differential phase eye diagram as received at the ONU. The eye diagram was constructed by sampling the input signal to the ONU coherent receiver ADCs in parallel with a high speed real time oscilloscope with 12.5 GSamples/s. The eye diagram was then constructed by offline down converting the recorded samples with a sine- and a cosine carrier, thus resulting in the I and Q components of the data, based on which the differential phase angles were calculated. This differential phase data was then sampled at the bit duration interval and a histogram showed the distribution of the differential phase angles within the sampling time. As the correct sampling time is unknown, a scan over all sampling times is performed and the resulting histograms for each time of sampling are plotted. The pseudo eye diagram is a very useful debug tool for DQPSK modulated signals.

Both OLT and ONU are real-time capable. To demonstrate this, the data stream of a High Definition Video Server has been sent though the OLT downstream to the ONU where the data stream was recovered and transmitted to a standard video decoder. Real time video was observed and the onset of macro blocking was seen when the ONU input power was reduced to below the video decoder's FEC level.

VII. Optical Front End

A simple UDWDM system where the OLT consists of a single OTG connecting to 10 ONUs can be readily implemented as all the design targets for such system have been met: OTG Tx power of -2 dBm/wavelength, OLT Rx sensitivity of -40 dBm, ONT Tx power of $+3$ dBm, and optical link budget of 43 dB. When multiple OTGs are present with a central frequency separation of 50 GHz, the resulting spectrum is illustrated by Fig. 13. As in Fig. 8 the tall central spikes represent the pilot tones. Despite of their peak amplitude, the energy content of the pilot tones is negligible as explained in Section V.

In order to demonstrate the full capacity of the system, a signal was generated by modulating 96 wavelengths from a laser bank (50 GHz grid) in one OTG. This generates 960 wavelengths shown in Fig. 13, each carrying 1.244 Gbit/s and transmitting a total capacity of 1.194 Tbit/s.

An optical front end is required to multiplex downstream signals from these OTGs and to de-multiplex upstream signals towards the respective target OTGs. Depending on the number of OTGs and the available ODN power budget, different designs of such an optical front end may be advantageous. Fig. 14 shows a generic configuration where the combining multiplexing elements can be power splitters, AWGs or a mixture. In order to compensate for the optical losses within those components, an optical amplifier is employed. As the OTGs are wavelength selective by virtue of coherent reception, the distribution of signals to the OTGs in the upstream direction can be performed by an arbitrary combination of splitters and AWGs, together with an optical amplifier to compensate the losses. Whether splitters, AWGs or a combination are used depends on the specific use case. Splitters offer low cost and high flexibility but may have higher insertion losses than AWGs. As a result, they may need a better and more expensive optical amplifier.

When the system operates with its full theoretical capacity of 1000 wavelengths, the total optical power into the fiber is $+28$ dBm which exceeds the eye safety regulation for class 1M laser. Therefore, an automatic laser shutdown circuit has to be installed for systems with more than 240 wavelengths and shuts down the downstream light in case of a fiber cut.

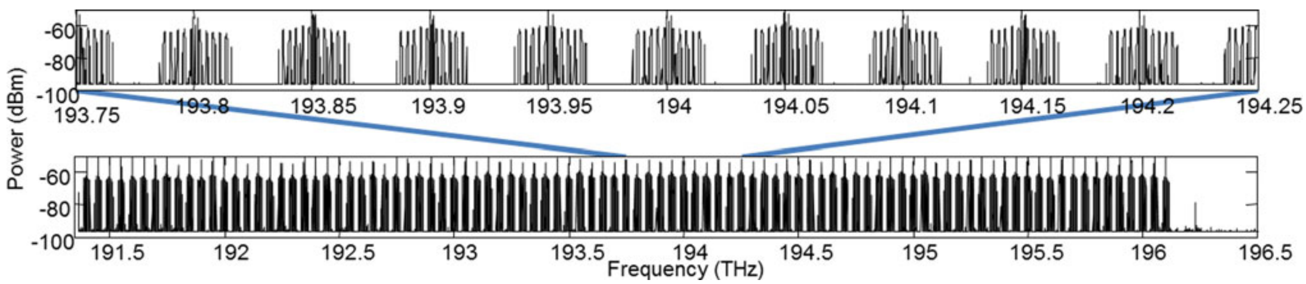

Fig. 13. 960 wavelengths demonstration.

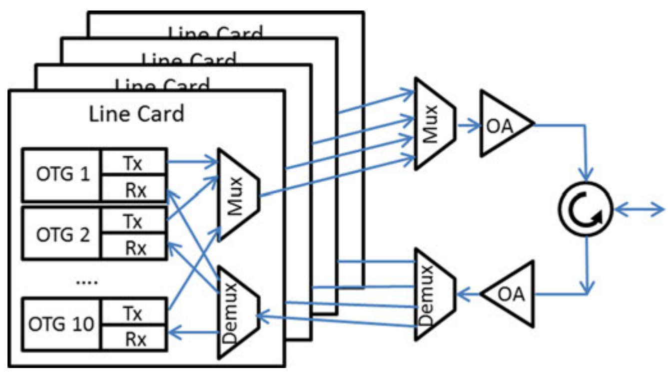

Fig. 14. Multiplex- and Demultiplexing stages at the OLT. OA: Optical Amplifier; Mux: either splitter or AWG, Demux: either splitter or AWG.

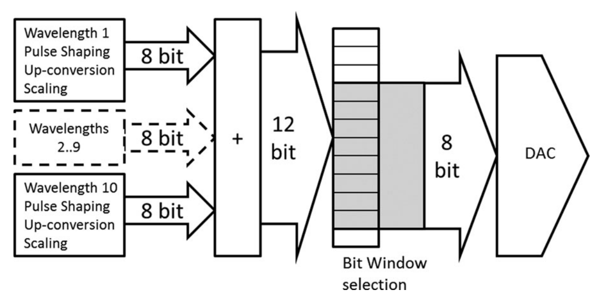

Fig. 15. DSP Carrier adding and bit selection stage.

VIII. Effects of 8 BIT DAC Resolution

The required high data rate of 60 GSamples/s makes the DAC a critical component of the OLT. From a signal quality point of view, a high DAC resolution is aspired. However, cost, complexity and power consumption demand a minimal resolution. This section describes how a compromise can be found.

The high speed DACs have a nominal resolution of 8 bit and an effective number of bits (ENOB) of 5.5–6 bits at 60 GSamples/s. On systems which generate multiple carriers with DACs, doubling the number of carriers requires an additional 0.5 ENOBs in order to keep a constant Signal to Noise Ratio (SNR). The SNR at the DAC output can be described as [20]:

$$\mathrm{SNR} = \mathrm{ENOB} \times 6.02\ \mathrm{dB} + 4.77\ \mathrm{dB} - 20 \times \log \frac{A_{\mathrm{peak}}}{A_{\mathrm{eff}}}. \quad (1)$$

Here, the peak and average amplitudes of the multicarrier sum signal are denoted by A_{peak} and A_{eff} respectively. The factor 6.02 comes from conversion of bit representation to decibel representation, and the term 4.77 dB comes from DAC quantization error. For sinusoidal signals with n carriers (e.g. phase modulated sinusoidal carriers), we have

$$\frac{A_{\mathrm{peak}}}{A_{\mathrm{eff}}} = \sqrt{2n} \quad (2)$$

Thus $\mathrm{SNR} = \mathrm{ENOB} \times 6.02\ \mathrm{dB} - 10 \log n + 1.76\ \mathrm{dB}$ proves the claimed relation. With 10 carriers, the ENOBs are reduced by $0.5 \times \log_2 10 = 1.7$ to about 3.8 ENOBs or an equivalent SNR of roughly 24.6 dB per carrier.

In order to deliver this SNR, the multi-carrier signal has to be composed in the right way. Fig. 15 shows the realization in the DSP block: each wavelength has an individual up-conversion and pulse forming stage, which also contain scaling units which allow scaling the carriers to arbitrary but constant amplitudes. Each of these stages delivers an 8 bit wide output bus. The effective size of the output depends on the scaling: for low scaling factors, only the least significant bits carry a signal while the most significant bits are set to zero. The 10 data buses, each 8 bit wide, are all added to form a 12 bit wide data bus.

As the DAC is limited to 8 bit bus width, a programmable bit window selector is set to capture the 8 most significant bits out of the 12 bit data bus. Fig. 15 shows only a single instance of the building block. In order to reduce the clock frequency of the DSP, the outputs of the Pulse Shaping and Up Conversion units have a width of 96×8 bits and the following adder and bit selection stages are 96 times parallel. The resulting SNR depends on the sequence of scaling, adding and truncating. To fully use the dynamic range of the DAC, the numerical values sent to the DAC ideally should cover the full range between -128 and 127 without exceeding it. For 4 carrier wavelengths, the first case is to scale each of the wavelengths to amplitude of 31 so that the total amplitude adds up to 124. The resulting optical spectrum of four wavelengths at the output of the IQ modulator in the OLT is shown in Fig. 16 (red curve). Although the SNR differs slightly from wavelength to wavelength, it is always $\sim$20 dB. The spectral component at 0 GHz is the OTG laser and the line at 933 MHz represents a pilot tone needed for the modulator control. The thin peaks between the modulated wavelengths are clock spur artifacts generated by the DAC.

By contrast, the black lines in Fig. 16 show the spectrum for the case that each of the four wavelengths was scaled to full amplitude and the resulting 10 bit signal was truncated by omitting the two least significant bits, i.e. only bits 2–8 are sent to the DAC. It can be seen that the modulated wavelengths are

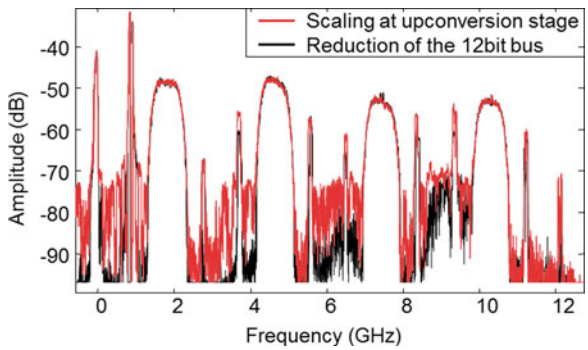

Fig. 16. Comparison of the SNR for different scaling and truncation strategies.

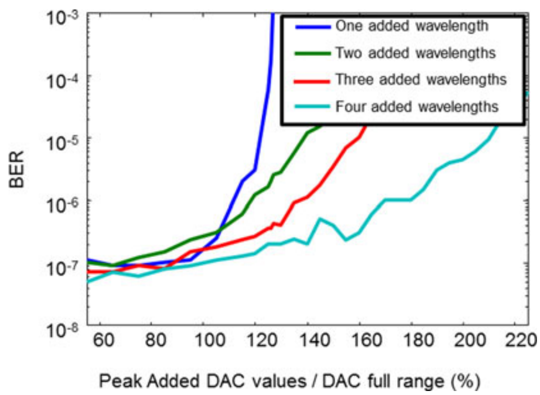

Fig. 17. Effect of clipping on the BER for different numbers of active wavelengths.

identical but that the quantization noise is about 10–20 dB lower than that in the first case. This is because the signal addition is done with greater accuracy (more significant bits) in the second case, which reduces the cumulative quantization error.

Note that the amplitudes of all carriers are chosen such that the DAC dos not saturate in any case. However, the bit window selector in Fig. 15 is built such that it does saturate, i.e., if any of the non-selected higher bits is set, the output of the bit window selector is 0xFF and the DAC output clips.

When many wavelengths are active, it is unlikely that all carriers simultaneously reach their maximum numerical value. In order to improve SNR from the quantization, it is favorable to increase the scaling of each carrier as much as possible, as Fig. 16 also shows. One can tolerate a few clipping events resulting in additional bit errors that can be corrected by the FEC.

As Fig. 17 shows, a higher number of carriers leads to fewer clipping events, as it is statistically expected. Therefore, with higher carrier counts, the scaling amplitude of the single carriers can be increased and rare clipping events can be tolerated.

In Fig. 17 BER was measured using one test wavelength. Then, 1–4 additional wavelengths were added such that the scaling amplitudes of all carriers were equal. The percentage of the added peak values relative to the DAC full range is given in the X-axis. Each wavelength carries a PRBS 15 signal. The influence of the statistics can be clearly seen: the more additional channels are active, the lower the penalty is. If for example a penalty from a BER of 10^{-7} to 10^{-6} is acceptable, a two channel system can be driven up to total DAC amplitude of about 110% while a 5 channel system can be driven to about 160%. Note that the percentages are estimates and not fully precise due to pulse shaping overshoot effects and the additional pilot tones for modulator control. Also, additional wavelengths slightly influence the RF drivers which explain the slight increase in BER for percentages below 100%.

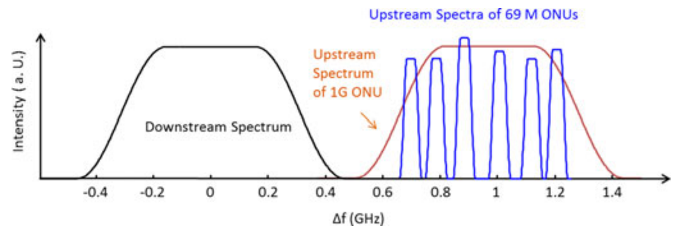

Fig. 18. Upstream wavelength assignment for the multiple ONUs per wavelength case.

IX. Bit Rate Flexibility

The system offers a wide span of sustained bit rates. Bit rates lower than 1.244 Gbit/s are realized by sharing one downstream wavelength among up to 6 ONUs in a Time Domain Multiplexed (TDM) manner. The upstream direction remains as WDMA. The available upstream spectrum is shared by up to 6 ONUs. By doing so, the disadvantages of a TDM upstream scheme, e.g., burst mode, dynamic bandwidth allocation protocols and related issues can be avoided. This is sketched in Fig. 18. Each of the upstream spectral bands represents a different ONU. As the LO lasers are not optically phase locked (see Section VI), guard bands are needed in between the ONU signals in order to avoid crosstalk. In short, up to 6 ONUs share a downstream wavelength via TDM (in downstream, TDM adds no significant penalty) and in upstream each of the ONUs still has its own WDM wavelengths.

For coherent transmission systems, the dependency of the possible symbol rate and the modulation format on laser linewidth has been shown in numerous publications [21]. The restricted upstream spectra per ONU (~70 MHz) operating at lower bit rates would require a laser linewidth on the order of a few 10 kHz to transmit QDPSK modulated data. Such a small laser linewidth is challenging in a cost sensitive system. In order to use the same 500 kHz linewidth laser, the modulation format is changed to on-off keying, resulting in an upstream data rate of 69 Mbit/s per ONU.

As the ONU uses an IQ-Modulator and the generation of the upstream light is software defined, the same ONU hardware can be used for a single 1.244 Gbit/s, or one or more 69 Mbit/s upstream signals.

Bit rates of, for example, 5 or 10 Gbit/s are realized by combining the wavelengths transmitted by one OTG and using a second OTG as an ONU. A 10 Gbit/s ONU thus uses the same hardware as an OTG in the OLT, and receives/transmits 10 wavelengths each at 1.244 Gbit/s simultaneously.

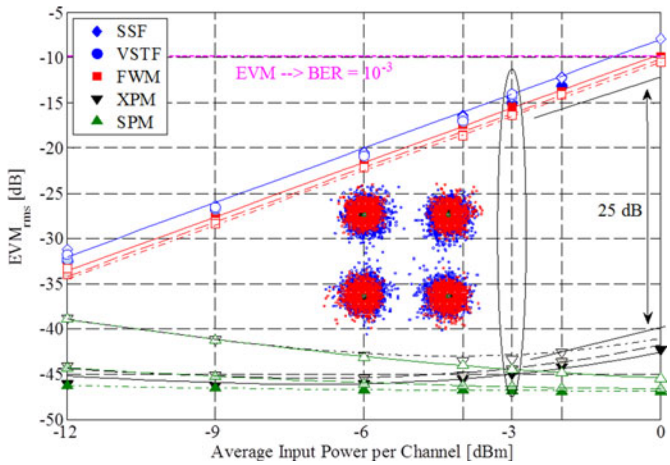

Fig. 19. EVM (center wavelength) versus input power for 32 × 1.25 Gbit/s (solid lines + filled markers: 25 km, dash lines + partially filled markers: 60 km, dash-dot lines + open markers: 100 km). Inset constellation (center wavelength) for -3 dBm at 25 km, considering SSF (blue) and FWM (red).

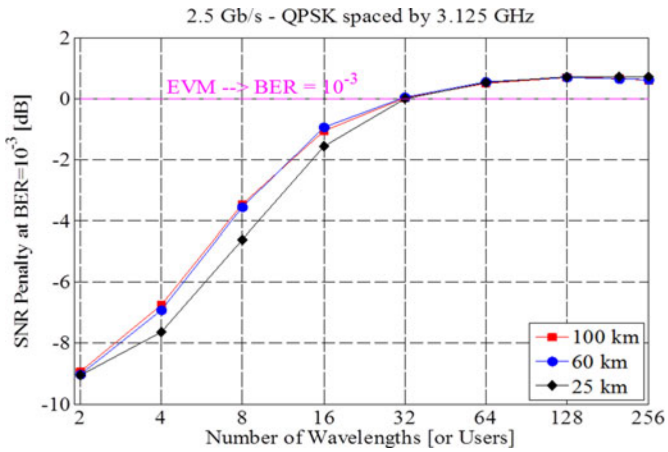

Fig. 20. SNR penalty at BER $= 10^{-3}$ (center wavelength) versus number of wavelengths in log scale spaced by 3.125 GHz for 2.5 Gbit/s.

X. UDWDM in the Fiber: Nonlinear Interaction Limits

The concept of UDWDM relies on feeding a high number of closely spaced wavelengths into the fiber plant. Fiber nonlinearities such as self-phase modulation (SPM), cross-phase modulation (XPM) and four-wave mixing (FWM) would limit the network's performance if the optical power is not properly optimized. In recent years, some works investigated fiber related impairments in UDWDM systems in which the network may operate at reduced symbol rate (e.g. 625 Mbaud), narrow wavelength spacing (e.g. 3 GHz), increased transmission distance (e.g. 100 km) and increased wavelength count (e.g. higher than 32).

Fig. 19, for example, depicts the Error Vector Magnitude (EVM) simulations of the center wavelength (worst case) for different conditions of input power, transmission distance and fiber nonlinearities. For these results the following fiber and simulation parameters were used: fiber loss of -0.2 dB/km, dispersion of 16.5 ps/nm/km, nonlinear coefficient of $1.35\text{W}^{-1}\text{km}^{-1}$, time window with 2^{18} samples (512 random symbols), 2^{14} (16384) simulated symbols. The blue line represents reference results obtained from the total field propagation using Split-Step Fourier (SSF) simulations (step size about 40 m), which accounts for all Kerr nonlinearities together. The calculation of fiber nonlinearities represented by green (SPM only), black (XPM only) and red (FWM only) results are based on Volterra Series Transfer Function (VSTF) [22]. The overall performance (blue results) indicates that fiber nonlinearities limit the feeder input power per wavelength below -2 dBm when the network transports 32 × 1.25 Gbit/s QPSK wavelengths equally spaced by 3.125 GHz. In order words, the EVM in dB increases with the square of power $(\text{EVM}_{\text{dB}} = 10 \times \log_{10}(P^2)$ and $\text{EVM}_{\text{dB}} = 10 \times \log_{10}(\text{EVM}^2_{\text{RMS}}))$ up to the limits of -9.8 dB (SNR≈9.8 dB) that corresponds theoretically to BER $= 10^{-3}$ for QPSK. By analyzing each nonlinear effect individually, it is clear that QPSK transmission is mostly impaired by FWM (highlighted in the inset constellation in Fig. 19) whose impact decreases with distance. The impact by XPM and SPM is almost 30 dB lower than that by FWM. In the case of SPM, this effect is even lower than the receiver sensitivity meaning that the EVM is reduced as the power is increased.

Besides power, it is also relevant to investigate the network's behavior for different number of wavelengths or total capacity.

Fig. 20 depicts the overall performance in terms of SNR penalty at BER $= 10^{-3}$ (center wavelength) using SSF simulations for up to 256 wavelengths, each at 2.5 Gbit/s with 3.125 GHz spacing.

Fiber and simulation parameters are similar to the previous ones used in Fig. 20, except the time window, which in this case corresponds to 1024 symbols (32,768 simulated symbols are used for estimating the performance). The SNR penalty is calculated from the actual EVM normalized by the theoretical EVM corresponding to BER $= 10^{-3}$.

In addition, the input power per wavelength was set so that the SNR penalty is 0 dB at 25 km of fiber. When the network transports only QPSK wavelengths, the SNR is penalized when the number of wavelengths increases to 32. Higher than 32 wavelengths, the performance remains unchanged (below 1 dB penalty) due to the sole effect of FWM being limited to around 100 GHz bandwidth (32 × 3.125 GHz). This indicates that in terms of nonlinearities, transmitting 1000 QPSK wavelengths gives similar nonlinear performance (about 0.8 dB penalty) as transmitting 32 QPSK wavelengths. Therefore, if the network is designed to support over a thousand users per fiber with data rates per user at a few Gbit/s, QPSK transmission is appropriate.

XI. Co-Existence With Legacy System: GPON, XG-PON and RF Video

One of the challenges of UDWDM systems is the coexistence with deployed PON technologies. To save wavelength spectrum, it is relevant to minimize the guard band to legacy technologies. On the other hand, reducing the guard band comes at a price of higher interference between different technologies sharing the

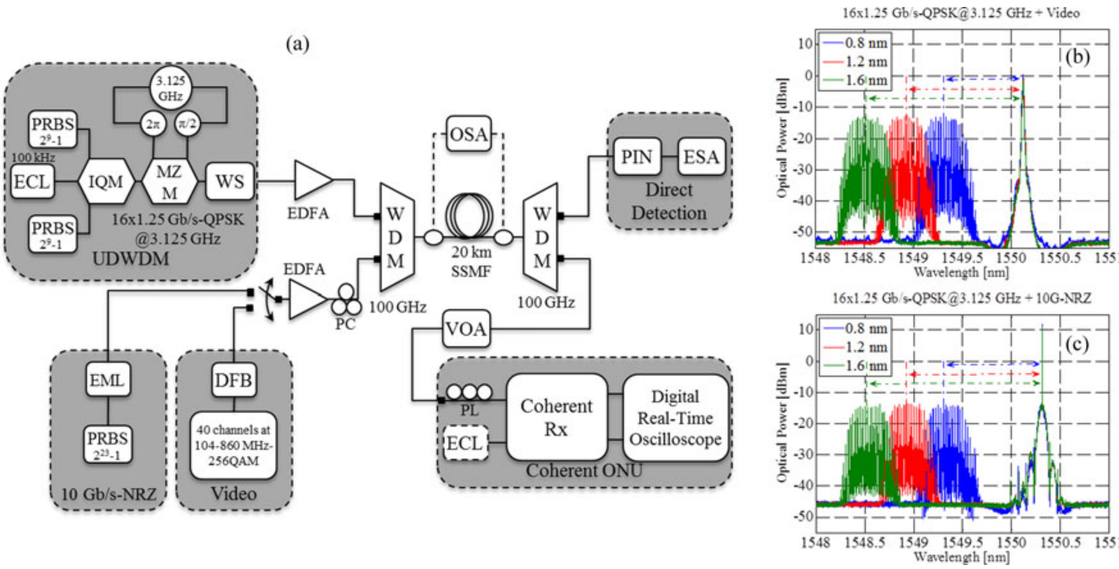

Fig. 21. (a) Experimental setup of UDWDM coexistent with legacy PON systems. PRBS: pseudo random binary sequence. ECL: external cavity laser. DFB: distributed feedback laser. EML: electro-absorption modulator integrated laser. IQM: IQ modulator. MZM: Mach-Zehnder modulator. WS: wave shaper. OSA: optical spectrum analyzer. ESA: electrical spectrum analyzer. PC: polarization controller. PL: Polarization locker. (b) Coexistence with digital Video. (c) Coexistence with 10G–NRZ.

same ODN. This interference is mostly induced by fiber nonlinearities such as FWM, XPM and SRS (Stimulated Raman Scattering) crosstalk. Therefore, it is of great significance to optimize both launched power and guard band so that those effects do not impair the quality of UDWDM wavelengths. UDWDM may also impair other deployed technologies (analog Video distribution for instance) via SRS effect as the work carried out in [23]. In this work we focused on the overall effect (Kerr nonlinearities and SRS) on the UDWDM wavelengths due to other coexisting wavelengths (G/XG-PON and Video overlay).

Fig. 21 depicts the experimental setup for analyzing the required guard band of heterogeneous network scenarios comprised of a UDWDM comb with 16×1.25 Gbit/s QPSK channels at $\sim$1549 nm and spaced by 3.125 GHz coexisting with either RF video at 1550.2 nm or 10 Gbit/s Non-Return to Zero (NRZ) systems at 1550.3 nm, whose optical powers scale up to 17 dBm. The performance is evaluated in both QPSK wavelengths (center wavelength) and RF video channel. Fig. 21(b) and (c) show the spectra of 16×1.25 Gbit/s–QPSK plus digital video and legacy PONs, respectively.

The results in Fig. 22 and Fig. 23 show that the EVM performance (center QPSK wavelength) does not change significantly for input power (video and 10 Gbit/s NRZ) ranging from 0 to 10 dBm. In this power regime, the performance is mostly limited by FWM among the -3 dBm QPSK wavelengths and an extra XPM penalty induced by the coexisting wavelength. As the input power increases to higher than 10 dBm, EVM rapidly reaches -9.8 dB (SNR $\approx$ 9.8 dB), represented by the magenta dash line (theoretical BER $= 10^{-3}$), at power around 16 dBm and 15 dBm, for the video and 10 Gbit/s NRZ wavelengths, respectively.

In this case, EVM in dB increases roughly with the square of input power, i.e. EVM increases by 2 dB for every 1 dB increase in the input power. This performance degradation is

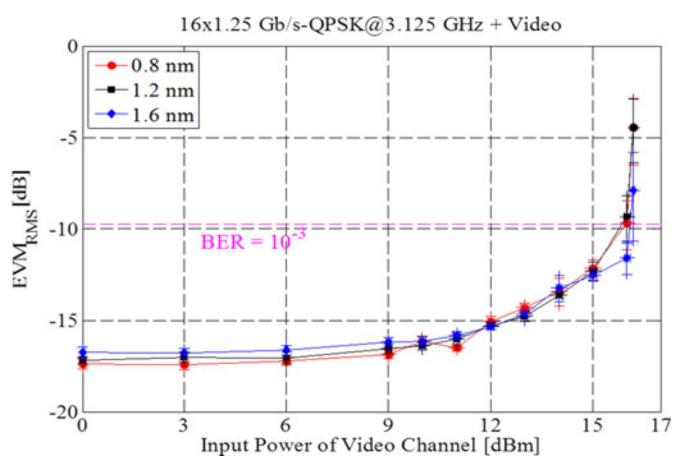

Fig. 22. EVM (center wavelength) after transmission over 20 km-SSMF versus input power of video channel.

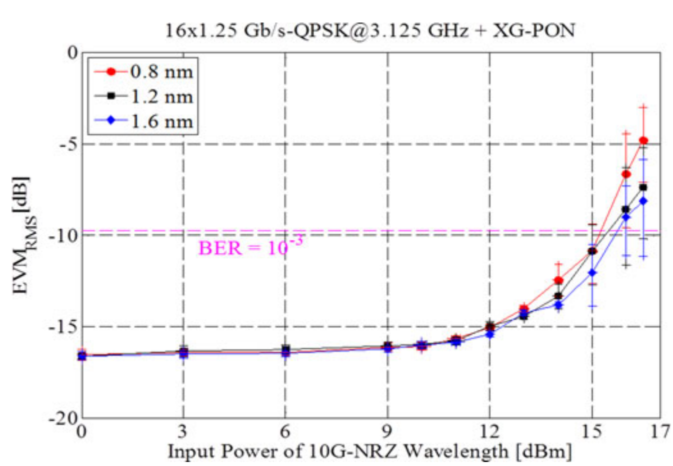

Fig. 23. EVM (center wavelength) after transmission over 20 km-SSMF versus input power of 10 Gbit/s-NRZ wavelength for three different guard bands.

due to inter-channel nonlinearities that induce both amplitude and phase noise in the recovered symbols. The EVM dependence on guard band is only noticeable for bands higher than 200 GHz (1.6 nm). Such a high power is particularly relevant since some PON technologies, as some XG-PON transmitter classes for instance, may operate at power as high as 16.5 dBm.

In summary, using DSP-based ONUs in UDWDM for transmission over 20 km of SSMF is successfully demonstrated considering guard bands of 0.8 nm (100 GHz), 1.2 nm (150 GHz) and 1.6 nm (200 GHz). Although the performance and impact of both Video and 10G–NRZ channels are not reported in this work, based on the findings of [23] and on the lab tests, we checked that the UDWDM comb does not impose significant interference in the aforementioned technologies if the power per channel is low (typically for the referred formats ~ -10 dBm).

XII. Summary and Outlook

This paper describes in detail an UDWDM system capable of providing up to 1000 wavelengths with variable data rates from 150 Mbit/s to 10 Gbit/s for up to 100 km reach in metro and access networks. It is also suitable for mobile front haul and mobile backhaul networks. An innovative PCT generates ultra dense wavelengths spaced at $\sim$3 GHz. The PCT utilizes the coherent reception and tunable laser to achieve the desired receiver sensitivity as well as the ultra dense wavelength spacing.

A demonstrator with 30 wavelengths (in groups of 10) was built and used as basis for the different experimental setups.

The full capacity of the downstream transmission was demonstrated by generating 960 wavelengths, each carrying 1.244 Gbit/s and transmitting a total capacity of 1.194 Tbit/s.

Block diagrams and operation details of real-time OLT and ONU implementations are discussed. In the OLT, a single laser source generates ten independently modulated DQPSK signal at 622 Mbaud through the use of DSP. In the ONU, a tunable laser is locked onto the downstream wavelength and serves as the upstream signal as well as the LO for downstream coherent reception. A receiver sensitivity of -48 dBm was demonstrated. Together with the FWM limited downstream power of -2 dBm per wavelength, an ODN power budget of 46 dB was demonstrated, which leaves 3 dB of margin with regard to the target loss budget of 43 dB.

The analysis of fiber nonlinearity on system performance shows that the limitation is predominately caused by FWM. When the wavelength count is higher than 32, the impact from FWM remains unchanged. Experimental results of coexistence of UDWDM with deployed systems confirm that DSP-based ONUs in UDWDM for transmission over 20 km of SSMF is possible with guard bands of only 0.8 nm (100 GHz), 1.2 nm (150 GHz) and 1.6 nm (200 GHz).

Coherent metro and access networks have been gaining attention, as numerous recent publications show [24], [25] and [26]. The main argument against the commercial deployment of coherent access and metro systems was, until now, the perceived high cost of coherent systems. However, recent technology advances in integrated CMOS Silicon photonics demonstrate the potential for high volume, cost effective optical modules [27]. This advance in Silicon photonics, in conjunction with cost effective DSP chips and efficient algorithms [28] renders the solution presented in this paper highly cost effective.

References

[1] T. Okoshi, "Recent advances in coherent optical fiber communication systems," *J. Lightw. Technol.*, vol. LT-5, no. 1, pp. 44–52, Jan. 1987.

[2] K. Kikuchi, "History of coherent optical communication and challenges for the future," in *Proc. IEEE Dig./LEOS Summer Topical Meeting*, Jul. 21–23, 2008, pp. 107–108.

[3] M. Nakazawa, K. Kikuchi, and T. Miyazaki, *High Spectral Density Optical Communication Technologies*. New York, NY, USA: Springer, 2010.

[4] H. Rohde, E. Gottwald, S. Smolorz, and K. Kloppe, "Next generation optical access: 1 Gbit/s for everyone," presented at the Eur. Conf. Exhib. Opt. Commun., Vienna, Austria, Sep. 20–24, 2009.

[5] Y. S. Kim, S. H. Lee, S. S. Lee, and J. L. Lee, "Upgrading WDM networks using ultradense WDM channel groups," *IEEE Photon. Technol. Lett.*, vol. 16, no. 8, pp. 1966–1968, Aug. 2004.

[6] E. J. Bachus, R. P. Braun, W. Eutin, E. Grossman, H. Foisel, K. Heimes, and B. Strebel, "Coherent optical-fiber subscriber line," *Electron. Lett.*, vol. 21, no. 25, pp. 1203–1205, Dec. 1985.

[7] L. Kazovsky, "Homodyne phase shift keying systems: past challenges and future opportunities," *J. Lightw. Technol.*, vol. 24, no. 12, pp. 4876–4884, Dec. 2005.

[8] J. Prat and J. Fabrega, "New homodyne receiver with electronic I and Q differential demodulation," presented at the Eur. Conf. Exhib. Opt. Commun., Glasgow, U.K., Sep. 25–30, 2005, Paper We4.P.104.

[9] C. Bock, J. Fabrega, and J. Prat, "Ultra-dense WDM PON based on homodyne detection and local oscillator reuse for upstream transmission," presented at the Eur. Conf. Exhib. Opt. Commun., Canes, France, Sep. 24–28, 2006, Paper We3.P.168.

[10] H. Rohde, E. Gottwald, P. Alves, C. Oliveira, I. Dedic, and T. Drenski, "Digital multi-wavelength generation and real time video transmission in a coherent ultra dense WDM PON," presented at the Opt. Fiber Commun. Conf., Anahaim, CA, USA, Mar. 17–21, 2013, Paper OM3H3.

[11] J. D. Reis and A. L. Teixera, "Architectural optimization of coherent ultra-dense WDM based optical access networks," presented at the Opt. Fiber Commun. Conf., Los Angeles, CA, USA, Mar. 6–10, 2011, Paper OTuB7.

[12] R. S. Luis, A. Shahpari, J. D. Reis, R. Ferreira, Z. Vujicic, B. J. Puttnam, J. Mendinueta, M. Lima, M. Nakamura, Y. Kamio, N. Wada, and A. Teixeira, "Ultra high capacity self-homodyne PON with simplified ONU and burst-mode upstream," *IEEE Photon. Technol. Lett.*, vol. 26, no. 7, pp. 686–689, Apr. 2014.

[13] D. Lavery, M. Paskov, and S. J. Savory, "Spectral shaping for mitigating backreflections in a bidirectional 10 Gbit/s coherent WDM-PON," presented at the Opt. Fiber Commun. Conf., Anahaim, CA, USA, Mar. 17–21, 2013, Paper OM2A6.

[14] S. J. Savory, "Digital coherent optical receivers: Algorithms and subsystems," *IEEE J. Sel. Topics Quantum Electron.*, vol. 16, no. 5, pp. 1164–1179, Oct. 2010.

[15] M. G. Taylor, "Phase estimation methods for optical coherent detection using digital signal processing," *J. Lightw. Technol.*, vol. 27, no. 7, pp. 901–914, Apr. 2009.

[16] H. Wang, Y. Lu, and X. Wang, "Channelized receiver with WOLA filterbank," in *Proc. Int. Conf. Radar*, Shanghai, China, Oct. 16–19, 2006, pp. 1–3.

[17] F. J. Harris, C. Dick, and M. Rice, "Digital receivers and transmitters using polyphase filter banks for wireless communications," *IEEE Trans. Microw. Theory Techn.*, vol. 51, no. 4, pp. 1395–1412, Apr. 2003.

[18] S. Smolorz, E. Gottwald, H. Rohde, D. Smith, and A. Poustie, "Demonstration of a coherent UDWDM-PON with real-time processing," presented at the Opt. Fiber Commun. Conf., Los Angeles, CA, USA, Mar. 6–10, 2011, Paper PDPD4.

[19] P. G. Goetz, H. Eisele, K. C. Syao, and P. Bhattacharya, "1.55 μm optical phase-locked loop with integrated p-i-n HBT photoreciever in a flexible development platform," *Microw. Opt. Technol. Lett.*, vol. 15, no. 1, pp. 4–7, May 1997.

[20] R. G. Lyons, *Understanding Digital Signal Processing*. Reading, MA, USA: Addison-Wesley, 1997.

[21] L. Kazovsky, G. Kalogerakis, and W. T. Shaw, "Homodyne phase-shift-keying systems: Past challenges and future opportunities," *J. Lightw. Technol.*, vol. 24, no. 12, pp. 4876–4884, Dec. 2006.

[22] J. D. Reis, D. M. Neves, and A. L. Teixera, "Analysis on nonlinearities on coherent ultra-dense WDM-PONs using volterra series," *J. Lightw. Technol.*, vol. 30, no. 2, pp. 234–241, Jan. 2012.

[23] A. Shahpari, J. D. Reis, S. Ziaie, R. Ferreira, M. J. Lima, A. N. Pinto, and A. Teixeira, "Multi system next-generation PONs impact on video overlay," presented at the Eur. Conf. Exhib. Opt. Commun., London, U.K., Sep. 22–26, 2013, Paper Tu.3.F.3.

[24] A. Shahpari, J. D. Reis, R. Ferreira, D. M. Neves, M. Lima, and A. N. Teixeira, "Terabit+ (192×10 Gb/s) nyquist shaped UDWDM coherent PON with upstream and downstream over a 12.8 nm band," presented at the Opt. Fiber Commun. Conf., CA, Mar. 17–21, 2013, Paper PDP5B3.

[25] R. Gaudino, "Advantages of coherent detection in reflective PONs," presented at the Opt. Fiber Commun. Conf., Anahaim, CA, USA, Mar. 2013, Paper OM2A1.

[26] C. Kottke, K. Habel, M. Eiselt, H. Griesser, and J. P. Elbers, "Coherent subcarrier-WDM-PON system with SSB modulation and wavelength reuse," presented at the Opt. Fiber Commun. Conf., Anahaim, CA, USA, Mar. 2013, Paper OM2A3.

[27] E. Marchens, T. Creazzo, S. B. Krasulik, P. K. L. Yu, D. Van Orden, J. Y. Spann, C. C. Blivin, J. M. Dallesasse, P. Varangis, R. J. Stone, and A. Mizrahi, "Integrated tunable CMOS laser for Si photonics," presented at the Opt. Fiber Commun. Conf., Anahaim, CA, USA, Mar. 2013, Paper PDP5C7.

[28] R. P. Giddings, "Real-time digital signal processing for future optical access networks," presented at the Opt. Fiber Commun. Conf., Anahaim, CA, USA, Mar. 2013, Paper OM3H5.

Harald Rohde received the Ph.D. degree in physics from the University in Innsbruck, Innsbruck, Austria, in 2001. Since then, he was with different departments of the Siemens AG, Nokia Siemens Networks, and Coriant. He worked on research for optical transmission systems, covering a broad range of topics. His current research interest include next generation optical access networks. He is author or coauthor of some 70 publications and holds more than 50 patents. He is actively involved in the standardization forum FSAN since 2008.

Erich Gottwald received the Dr. rer. nat. degree in physics in 1985. He joined Siemens Central Research Labs for Communication Technology in 1985. In the late eighties, he worked on coherent optical transmission systems and optical measurement techniques. With the up-coming of EDFAs, he switched to WDM systems in 1991 and, as suitable commercial simulation tools were not available at that time, developed a simulation tool for nonlinear fiber optical transmission systems. Besides that he was engaged in analog video transmission and ultrahigh data rate transmission. In the last years, he was engaged in coherent networks with ultradense channel spacing and system simulation.

Antonio Teixeira received the M.Sc. degree in 1994, and the Ph.D. degree in electrical engineering in 1999, all from the University of Aveiro, Aveiro, Portugal. He is currently an Associate Professor at the Department of Electronics, Telecommunications and Informatics, University of Aveiro and a Researcher at the Instituto de Telecomunicações, Aveiro. Dr. Teixeira is a member of the Optical Society of America, TPC of major conferences like OFC and ECOC, and several other conferences like ICTON, Networks, and GLOBECOM. He has more than 100 pier reviewed journal papers and more than 300 conference papers. He is the editor of several books and Optics Express; he has tutored more than 60 students (more than 15 Ph.D. and four Postdoctoral researchers). He worked with Nokia Siemens Networks and Coriant as a Senior Specialist on access networks in IEEE standards association and FSAN/ITU-T Q2 and Q6.

Jacklyn Dias Reis received the B.Sc. and M.Sc. degrees in electrical engineering with emphasis on telecommunications from Universidade Federal do Pará, Soure, Brazil, in 2005 and 2007, respectively. He received the Ph.D. degree in electrical engineering/telecommunications (*cum laude*) from the University of Aveiro, Aveiro, Portugal, in 2012. He was a Researcher from 2007 to 2013 at Instituto de Telecomunicações—Aveiro, focusing on optical communications, passive optical networks, next generation optical access networks, coherent optical communications, advanced modulation formats, digital signal processing, nonlinear optics and optimization techniques. He is currently working at CPqD, Campinas - SP, Brazil as the Senior Researcher in the division of optical technologies. He has published more than 50 papers, including journals and international conferences. Dr. Reis is a Member of the Optical Society of America.

Ali Shahpari received the M.Sc. degree in electrical engineering—telecommunications from Shiraz University, Shiraz, Iran, in 2003. He has been working toward the Ph.D. degree at the University of Aveiro, Aveiro, Portugal, and Instituto de Telecomunicações, Lisbon, Portugal, since 2010. His research topics include techno-economic and energy efficiency in next-generation optical access networks, free-space optics communication, and optical modulation formats using coherent and direct detection receivers. He has participated in several national (FCT and QREN support) and international projects included in the European Union Telecommunications R&D Programs: ACTS and IST.

Klaus Pulverer received the Ph.D. degree in mathematical physics from the University of Oxford, Oxford, U.K. After several years of research in mathematical modeling and numerical simulation at the Technical University of Munich, he joined Siemens and later Nokia Siemens Networks and Coriant to work in the fields of communication protocols, next generation networks architectures and optical access. He has been active in standardization since 2002, until 2008 as co-chair of architecture in ETSI TISPAN and afterward in ITU-T and FSAN for optical access.

Jun Shan Wey received the Ph.D. degree in high-speed optical communications from the University of Maryland, College Park, MD, USA. After receiving the Ph.D. degree, she held several research positions in both academia and industry on optical signal processing and optical wireless networks. After joining Siemens in 2004, subsequently Nokia Siemens Networks and Coriant, she was involved in IPTV product development and optical access networks. She is currently with the CTO Office—Network Architecture team. She is Coriant's delegation lead in FSAN and ITU-T Q2/SG15 and a coeditor of G.989.2 Recommendation.